Statistical inference of body representation in the macaque brain

Wen Fang[a,b,c], Junru Li[a,b], Guangyao Qi[a,d], Shenghao Li[a,d], Mariano Sigman[e,f], and Liping Wang[a,b,1]

[a]Institute of Neuroscience, Key Laboratory of Primate Neurobiology, Chinese Academy of Sciences (CAS) Center for Excellence in Brain Science and Intelligence Technology, Chinese Academy of Sciences, 200031 Shanghai, China; [b]Shanghai Center for Brain Science and Brain-Inspired Intelligence Technology, 201210 Shanghai, China; [c]Key Laboratory of Brain Functional Genomics, Institute of Cognitive Neuroscience, School of Psychology and Cognitive Science, East China Normal University, 200062 Shanghai, China; [d]University of Chinese Academy of Sciences, 100049 Beijing, China; [e]Laboratory Neuroscience, Universidad Torcuato di Tella, C1428 Buenos Aires, Argentina; and [f]School of Language and Education, Universidad Nebrija, 28015 Madrid, Spain

Edited by Ranulfo Romo, National Autonomous University of Mexico, Mexico City, D.F., Mexico, and approved August 5, 2019 (received for review February 8, 2019)

The sense of one's own body is a pillar of self-consciousness and could be investigated by inducing human illusions of artificial objects as part of the self. Here, we present a nonhuman primate version of a rubber-hand illusion that allowed us to determine its computational and neuronal mechanisms. We implemented a video-based system in a reaching task in monkeys and combined a casual inference model to establish an objective and quantitative signature for the monkey's body representation. Similar to humans, monkeys were more likely to perceive an external object as part of the self when the dynamics (spatial disparity) and the features (shape and structure) of visual (V) input was closer to proprioceptive (P) signals. Neural signals in the monkey's premotor cortex reflected the strength of illusion and the likelihood of misattributing the illusory hand to oneself, thus, revealing a cortical representation of body ownership.

body representation | causal inference | monkey | premotor | ownership

One of the fundamental elements of self-consciousness is the ownership of one's own body (1, 2). In everyday life, understanding the limits of our own body is an automatic and mostly flawless computation. However, experimentally, one can induce human body illusions in which inanimate objects are ascribed with ownership and perceived as part of the self (2). For instance, watching a rubber hand being stroked while one's own unseen hand is synchronously stroked induces a relocation of the perception of one's own hand toward the rubber hand (3), termed the rubber-hand illusion (RHI). There are different models of body illusion, and many of them agree on including multisensory integration as a key mechanism (1, 4). The perception of real and illusory arms largely relies on the integration of V, tactile and P signals, which are governed by principles of temporal and spatial congruencies (2, 5–8). Although remarkable advances have been made over past decades in our understanding of RHI through human behavioral and functional imaging studies (5, 9, 10), neurophysiological and computational mechanisms which give rise to this illusion have been comparatively significantly less investigated and understood.

In the process of building representations of the bodily self, the brain combines, in a near-optimal manner, information from multiple sensory channels. Entities in the outside world produce correlated noisy signals, and the brain combines this information to infer properties of this entity (2, 11), based on the quality and reliability of sensory stimuli (12). However, when superposing stimuli become sufficiently dissimilar and uncorrelated, the brain's inferential process of integration breaks down, leading to the perception that these stimuli originate in distinct entities. This sequential process of inferring first whether sources are assigned to the same entity or not and, subsequently, use this information downstream to integrate or segregate sensory inputs can be described quantitatively by the Bayesian causal inference (BCI) model (13–15), which has been proposed as a conceptual framework of body representation (2, 15). Yet, how the brain achieves the statistical inference of the cause from multiple sensory signals to form body representations remains largely unknown. Therefore, a nonhuman primate behavioral model of body representation would allow us to examine how single neurons implement computational components of BCI for the body ownership.

In this study, we designed a video-based system in a reaching task using a version of a moving rubber-hand illusion paradigm (16). The experimental system allowed us to parametrically increase the spatial distance between V and P signals and to replace the illusory (V) arm with nonhomomorphic objects in order to create the scenarios of incompatible VP inputs (16, 17). We then implemented a BCI model that allowed us to: 1) establish a computational estimate of the likelihood of integrating the V (artificial) and the P information, 2) build up an objective and quantitative proxy for the body ownership in macaques, and 3) use this signature to investigate, in a quantitative manner, the neuronal encoding of body ownership in the macaque brain.

Results

Paradigm for Studying Body Representation in Humans and Monkeys. We first asked 25 human subjects and trained 4 monkeys to reach a V target with their invisible P (self) arm, while viewing the V (illusory) arm moving in synchrony with a preset spatial VP disparity (Fig. 1*A*). In 1 trial, subjects were required to initiate the trial by placing their hand on the starting position (blue dot)

Significance

How humans and potentially other animals construct the experience of "being a self" remains one of the most intriguing questions in neuroscience. Over the past years, substantial advances have been made in understanding psychological mechanisms of bodily self through experimental manipulations in humans, such as rubber-hand illusion in which arbitrary objects may be ascribed with ownership and perceived as part of the self. The present study provides a demonstration in macaque monkeys and establishes objective and quantitative signatures of body representation at a single-trial level. Furthermore, we show that neural signals in macaque's premotor cortex reflect the strength of illusion and the likelihood of misattributing the illusory arm to oneself, thus, revealing a cortical representation of bodily self-consciousness.

Author contributions: W.F. and L.W. designed research; W.F., G.Q., S.L., and L.W. performed research; M.S. and L.W. contributed new reagents/analytic tools; W.F., J.L., and L.W. analyzed data; and W.F., J.L., M.S., and L.W. wrote the paper.

The authors declare no conflict of interest.

This article is a PNAS Direct Submission.

See Commentary on page 19771.

[1]To whom correspondence may be addressed. Email: liping.wang@ion.ac.cn.

This article contains supporting information online at www.pnas.org/lookup/suppl/doi:10.1073/pnas.1902334116/-/DCSupplemental.

First published September 3, 2019.

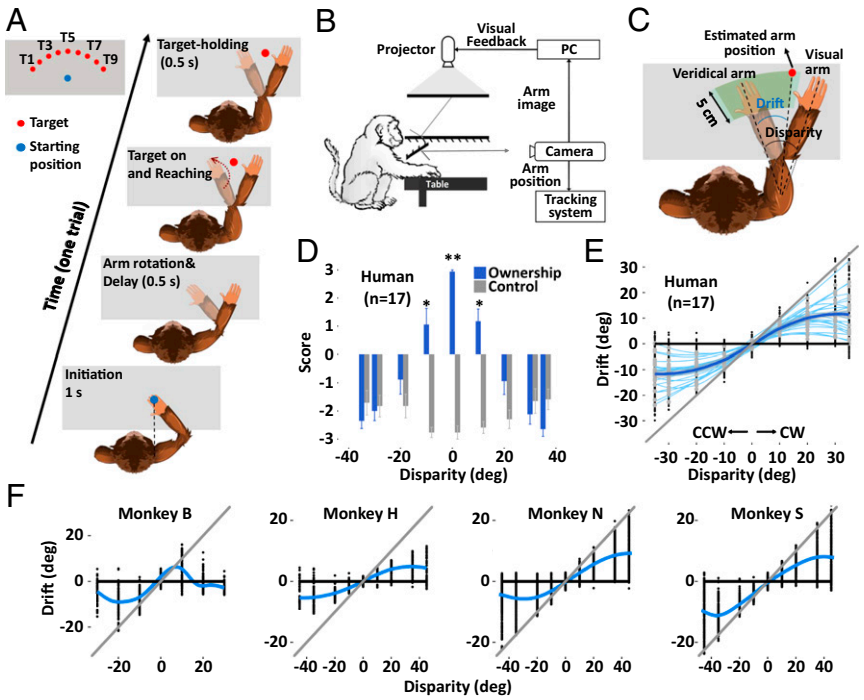

Fig. 1. Behavioral task, subjective illusion statements, and proprioceptive drift. (*A*) Overview of the task. The subject was instructed to hold its P hand over the starting position (blue dot) to initiate a trial. After the rotation of the V arm, a virtual red dot was presented, and participants were required to place their P arm on the target and hold to get a reward. (*B*) The video-based experimental system. (*C*) Schematic depicting "proprioceptive drift," and reward area (in green) for reaching to ensure that no feedback was given to monkeys about their response. The monkey was rewarded when the estimation of the arm was located anywhere between the positions of the pure V arm (completely bias to the V information, corresponding to the leftmost side of the green zone) and the pure P arm (completely bias to the P arm, the rightmost side of zone). The arm location displayed is an example trial with the disparity at +35° during the target-holding period. See also *SI Appendix*. (*D* and *E*) The subjective statements of arm illusion and proprioceptive drifts of 17 human participants (experiment 1, ownership and control questions see *SI Appendix*, Table S1). (*F*) proprioceptive drifts of 4 macaque monkeys (individual sessions see *SI Appendix*, Fig. S1). The absolute V (gray line) and P (black line) biases are also plotted. $*P < 0.05$; $**P < 0.01$.

for 1 s and were instructed not to move. After the initiation period, the starting point disappeared and the virtual (V) arm was rotated (*SI Appendix*), and this mismatch arm was maintained for 0.5 s as the "preparation period." The reaching target was presented as a "go" signal, and subjects had to reach to the V target (chosen from T1 to T9 randomly trial by trial, Fig. 1*A*) within 2.5 s and place their hand in the target area for 0.5 s ("target-holding period," monkeys received a reward for doing so). Any arm movement during the target-holding period automatically terminated the trial. Reaching was rewarded as correct when the V target ("the estimated arm") was located anywhere between the positions of the subject's P arm and the V arm, thus avoiding any bias as the subject was free to respond with either the self or the illusory arm (green zone in Fig. 1*C*, see details of animal training in *SI Appendix*). The proprioceptive drift due to the presence of the illusory arm, a behavioral correlate of the sense of arm ownership (3, 17), was measured at the endpoint of reach (target-holding period) and was defined as the angle difference between the P arm and the V target (the estimated arm) (Fig. 1*C*).

To investigate whether the hierarchical BCI model could be used to establish a direct relation between perceived ownership and spatial drift, we asked human participants to complete a standard questionnaire reporting their subjective ratings of arm ownership in another experiment in which the trials with the same disparity were grouped into 10-trial miniblocks (*SI Appendix*, Table S1 and *SI Appendix*). Analysis of the ratings showed that participants perceived the illusion (that the artificial arm was their own) when the VP disparity was small (≤10°) (0° and ±10°, 1-sample t test relative to 0, $P < 0.05$). The illusion progressively vanished when the disparity was larger than 20° (Fig. 1*D*). The measured proprioceptive drifts in humans showed a very similar pattern—increased for small levels of disparity and plateaued or even decreased when the disparity exceeded 20° (Fig. 1*E*). Importantly, the measurements on the 4 monkeys also showed a similar pattern of drifts (Fig. 1*F* and *SI Appendix*, Fig. S1, the disparity of ±90° was also tested in monkeys H, N, and S).

Hierarchical BCI Model Accounts for Proprioceptive Drifts. The BCI model can qualitatively explain the nonlinear dependence of drift as a function of disparity. For small disparities, the P and V signals have a high probability to arise from the same source. Hence, the V information is fully integrated (indicating that the artificial arm is owned) with a linear dependence on VP disparity. For large disparities, however, V and P signals are unlikely to arise from a single source, leading to a breakdown of integration and illusion. In this case, mostly P information is considered, and V information has a very weak weight in the integration process. As a consequence, the effect of disparity on drift is reduced.

To examine this hypothesis in a quantitative manner, we implemented the BCI model and used the "posterior probability of common source" (P_{com}), the consequence of causal inference, as a quantitative proxy of arm ownership. The model included, as free parameters, VP variances and "prior probability of common source" (P_{prior})—the preexisting knowledge for the inference—to account for the variability in spatial drifts observed in both humans and monkeys (Fig. 2 *A* and *B* and *SI Appendix*, Table S2, fitting for individual monkeys, see *SI Appendix*, Fig. S2). Results showed that the dependence of P_{com} on the disparity closely mimicked the profile of the rating of arm illusion in humans (Fig. 2 *C*–*E*; see results of individuals in Fig. 2*I* and *SI Appendix*, Fig. S3). The ownership index was defined as the half full width at half maximum (HWHM) of ownership rating curves. The model also accounted for individual human variability in arm ownership. The index of arm ownership (i.e., the disparity at which

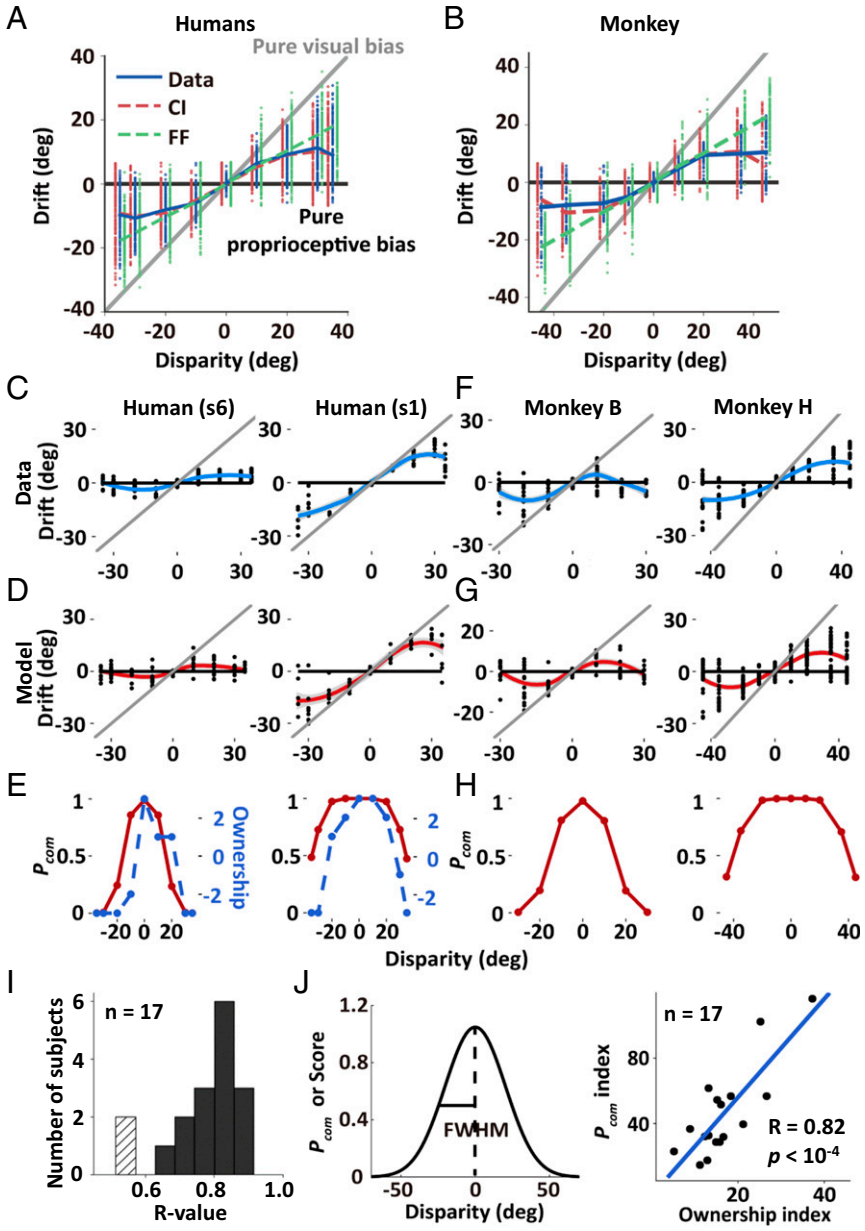

Fig. 2. BCI model fitting and arm ownership predicted by common source probability in both humans and monkeys. (*A* and *B*) The behavioral data (sessions' means and distribution across trials for monkey H [Fig. 1*F*] and subjects' means and distribution across trials for humans [$n = 17$, human experiment 1, see task procedure], in blue), and the predictions of the BCI model (in red) and the FF model (in green) (for histograms of model fittings and model comparison, see *SI Appendix*, Fig. S2 and Table S2 and *SI Appendix*). The absolute V (gray line) and P (black line) biases are also plotted. (*C* and *D*) Behavioral responses (each dot indicates 1 trial) and modal fittings (each dot indicates 1 simulated trial) from 2 example human participants (see all of the human data in *SI Appendix*, Fig. S3*A*). (*E*) The comparison of posterior common source probabilities (P_{com}, red lines) and illusion statements (ownership, blue dashed lines) for individual human participants (*SI Appendix*, Fig. S3*B*). (*F*–*H*) Plotted proprioceptive drift; model fitting, and P_{com} are shown for individual experimental sessions from monkeys B and H (see all of the monkey data in *SI Appendix*, Fig. S2). (*I*) Histogram of *the R* value (correlation between P_{com} and ownership score within subjects) of all human subjects. Fifteen (dark bars) out of 17 subjects showed the significant correlation (Pearson correlation, $P < 0.05$). (*J*) The ownership index was significantly correlated with the P_{com} across subjects. The ownership index and the common source probability index were defined as the HWHM of the respective curves (*SI Appendix*, Fig. S3*B*).

each participant had a 50% strength of the illusion) highly correlated with the equivalent estimate of P_{com} as a function of disparity (Fig. 2*J*, Pearson correlation, $R = 0.82$, $P < 10^{-4}$). A more taxing test for the BCI model is to compare its efficacy with a simpler model by which information is always combined optimally (assuming by default a common source). Model comparison showed that the BCI model significantly outperformed the forced-fusion (FF) model (*SI Appendix*, Table S2 and *SI Appendix*).

To summarize the above results: First, we found that the patterns of drift and of P_{com} in monkeys and humans showed a similar dependency on the disparity between P and V information. Second, in humans, the inferred likelihood that P and V information originated from the same (own) source (P_{com}) was tightly correlated with subjective reports of ownership. Thus, differing from previous animal studies using only passive visual exposure to a fake arm without any behavioral readout (6, 7, 18), we established a link between subjective measures of ownership (which cannot be measured directly in monkeys) and objective measures of drift distribution. This, in turn, allowed us to examine putative neural mechanisms underlying body representation in monkeys.

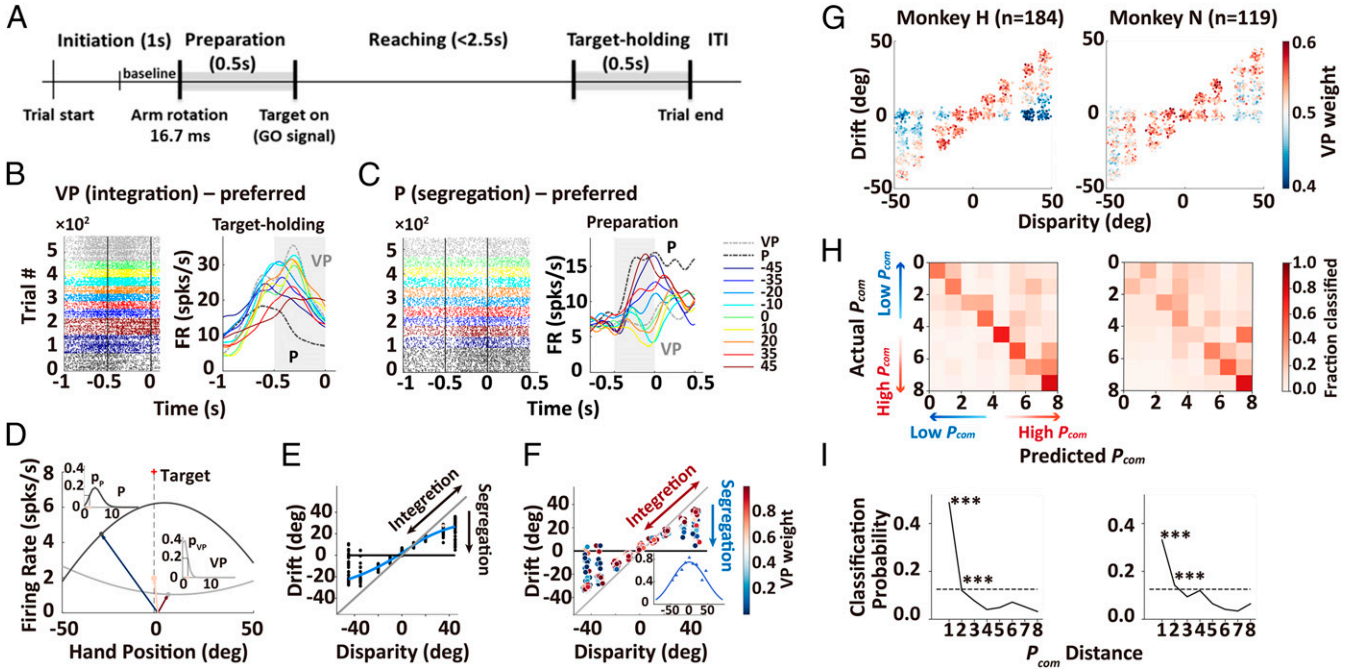

Fig. 3. Premotor neurons represent the posterior probability of the common source. (*A*) Sequence of events during a trial. (*B* and *C*) Rasters and histograms of activities from 2 example premotor neurons that exhibited responses varied with cue disparity that preferred to the VP or P condition during the target-holding and preparation periods (gray zones). (*D*) Diagram of probabilistic decoding analysis (see *Methods*) in 1 example trial in *E*. For a given spatial target (estimated arm, pink arrow) in a single trial of VPC (VP conflict) condition, the P arm (blue arrow) and the illusive V arm (red arrow) position were mapped onto the VP (gray curve) and P (black curve) tuning curves, respectively, to get the likelihoods. (*E* and *F*) Plotted proprioceptive drifts in the behavior of 1 example neuron and probability of VP (integration) under each disparity at the single-trial level (each dot in *F* indicates the corresponding trial in *E*). The *Inset* indicates the VP weight as a function of disparity. (*G*) CI pattern in the population neural activity from 2 monkeys during the target-holding period. For display, the trials with continuous drifts were divided into 29 clusters (*SI Appendix*, *Methods*). (*H*) Confusion matrices from 2 monkeys, derived when training a SVM on VP weights during the target-holding period. Values on the main diagonal represent correct classification. (*I*) Classification probability as a function of P_{com} distance. The dashed line represents chance level; asterisks represent significant differences between adjacent P_{com} distances. ***$P < 0.001$.

Neuronal Activities in the Premotor Cortex Encode the Strength of the Illusion. We recorded a total of 518 single neurons from the premotor cortex of 2 monkeys while performing the above reaching task. The recording chamber covered both dorsal and ventral premotor cortices, which were divided by the spur of the arcuate sulcus (297 from monkey H and 221 from monkey N; *SI Appendix*, Fig. S4 and *Methods*) (6). We chose to record from this area because previous studies have shown that it is involved in functions which are close to those required for developing arm ownership, specifically: 1) both medial and lateral parts of the premotor cortex are involved in the convergence of V and P cues during the monkey's arm movements (6), 2) these regions are involved in sharing sensory information across modalities, both in movement and in memory tasks (19, 20), and human functional imaging studies have shown the relevance of these areas in the processing of human arm ownership (5, 10). Before investigating neural responses when there are disparities between V and P information (for the VP-conflict [VPC]) task, we conducted 2 control experiments to characterize neural responses: 1) when V and P information are perfectly aligned (VP task) and 2) when there is only a P signal (P task) (*SI Appendix*). These 2 tasks involved expected stereotypical behaviors in 2 extreme regimes. Thus, neurons that are more active during the VP task reflect a preference for integrating congruent VP information and, hence, constitute a natural candidate for "*integration (VP)* neurons" (example in Fig. 3*B*). By contrast, neurons that are more active during the P task are likely candidates for "*segregation (P)* neurons" (Fig. 3*C*). We, therefore, predicted that, on a trial-by-trial basis, the similarity of neural responses during the VPC task to that of the VP or P tasks would predict whether monkeys integrated or segregated the illusory V signal and the P arm. We implemented a linear probabilistic model which combined, for each neuron and trial, how its response pattern aligned with the VP (λ_{VP}) and P (λ_P) response profiles and used this model to implement a probabilistic decoding analysis to calculate the probability of VP or P, based on the firing rate in each trial (Fig. 3*D* and *SI Appendix*).

We analyzed neural activities during the target-holding period, a segment of the task in which neural activities were not contaminated by movement artifacts (Fig. 3*A*). As shown in the behavioral analysis, the probability of integration decreased for greater disparities. Furthermore, at larger disparities (>30°), spatial drifts displayed a great variability across trials that went all the way from perfect integration (large drift, suggesting that, in these trials, monkeys attributed the illusory arm) to complete segregation (small drift in which V signal was much less integrated). Recordings from 303 neurons in 2 monkeys showing task-selective activities (155 VP and 148 P neurons) during the target-holding period were included in this analysis (*SI Appendix*, *Methods*). Fig. 3 *E* and *F* show the drifts in behavior and corresponding VP weights ($P_{VP}/[P_{VP} + P_P]$) of neural activities in single trials of 1 example neuron (for raster plots and histograms, see also *SI Appendix*, Fig. S5*A*). Specifically, the VP weight of the neuron progressively decreased along with the disparity (*Insets* of Fig. 3*F*) and in trials with large disparities (e.g., 35° and 45°), this example neuron had higher VP weights when the drift was large (i.e., the monkey integrated the illusive V arm) and shifted gradually toward higher P weights when the drift shifted to 0 (i.e., the monkey segregated the V information and lost the V arm ownership). A considerable number of neurons was found to correlate with the pattern of P_{com} obtained by fitting with drifts from the BCI model (79 out of 303, 26.1%, Pearson correlation between VP weight and P_{com} of 29 clusters, $P < 0.05$, *SI Appendix*, Fig. S5*B*) during the target-holding period, demonstrating that the dynamics of integration and segregation, the hallmark of causal

inference (CI) (13), was represented by single neuron activities at the single-trial level.

We next examined neuronal activities at the population level and asked whether its dynamics, potentially revealing nonlinearity, reflected the pattern of P_{com} revealed by the model. Fig. 3*G* shows that the same pattern of VP weights was observed when we pooled all 303 neurons in the analysis (linear regression, $P < 10^{-4}$). The changes in VP weights in the neuronal population closely fitted with the profile of the P_{com} obtained from patterns of drift (*SI Appendix*, Fig. S6, linear regression, monkey H: $R = 0.93$, $P < 0.001$; monkey N: $R = 0.93$, $P < 0.001$). As a control, we verified that the same neuronal population did not show any significant correlation with this pattern during the baseline period (*SI Appendix*, Fig. S7*A*). Furthermore, the pattern of VP weights in the neuronal population could not be explained by other task factors (e.g., positions of P, V arm, or eye fixation, *SI Appendix*, Fig. S7*B*).

Thus far, the analysis was performed within a range of disparities in which the probability of integration never vanished to 0. We then performed an experiment, where 66 neurons were recorded with 90° disparity (*SI Appendix*, Fig. S8*A*), a regime in which P_{com} is predicted to be minimal. Indeed, we found that neuronal activities for these trials with 90° disparity showed the lowest VP weights (similar to those of P neurons) (*SI Appendix*, Fig. S8*B*), indicating full segregation of VP signals.

To further test the relation between neural activity and behavior in a quantitative manner, we examined whether the population activities of these neurons can predict the likelihood that the monkey perceives the illusion. We trained a linear multiclass support vector machine (SVM), using pooled activities across recording sessions from 2 individual monkeys. The decoder was trained to identify 8 different bins of P_{com} (and, hence, the chance level was at 12.5%) with 3-fold cross-validation, and the significance was evaluated using a permutation method (*SI Appendix*, *Methods*). The results showed a significant decoding accuracy for P_{com} in the target-holding period (mean accuracy: H, 48.7%, $P < 0.001$; N, 33.6%, $P < 0.001$) (Fig. 3*H*). Furthermore, this analysis not only yielded high decoding accuracy, but also showed continuity in errors as revealed by the confusion matrix, i.e., errors were typically mapped to close neighbors (Fig. 3*I*). Using the activities of the same population of neurons during the baseline period, we verified that the decoding accuracy was not significantly above the chance level (mean accuracy: H, 17.6%, $P > 0.05$; N: 14.0%, $P > 0.24$).

Prior Knowledge of Body Representation Modulates Causal Inference. Previous studies have shown that the attributes leading to the assimilation of an entity as an owned body part involves not only integration of external sensory information, but also internal prior knowledge of preexisting body representation (21–24). Thus, in the BCI model, if the V arm is replaced by an object that does not match the features of an arm, the prior probability of common source (P_{prior}) should drop, leading to the decrease in the posterior probability (P_{com}). Additionally, this should, in turn, be reflected as a major shift of neuronal activities toward P neurons.

To test this prediction, we performed experiments using a piece of rectangular wood (of the same size) instead of the V arm (Fig. 4*A*). We found that the subjective ownership ratings (in humans) in the wood condition were significantly reduced as compared to those found in the V arm experiments (Fig. 4*B*, repeated-measures ANOVA, $P < 0.01$; post hoc test: at 0°: $P < 0.05$; at 10°: $P = 0.075$). For the measurements of proprioceptive drifts in both humans and monkeys, we found very similar reduction in the wood experiments (Fig. 4*C*, 2-way ANOVA; main effect of *Experiment*, $ps < 10^{-5}$), demonstrating a breakdown of arm illusion under the wood condition even for small disparity. By fitting behavioral data with the BCI model, we showed that the P_{prior} (Fig. 4 *D* and *E*, paired *t* test; $ps < 10^{-4}$) and P_{com} ($ps < 0.005$) were both significantly reduced in the wood condition. Furthermore, the decrease in P_{com} index was significantly correlated with the decrease in the ownership index between the arm and the wood conditions (*SI Appendix*, Fig. S10, $R = 0.59$, $P < 0.01$).

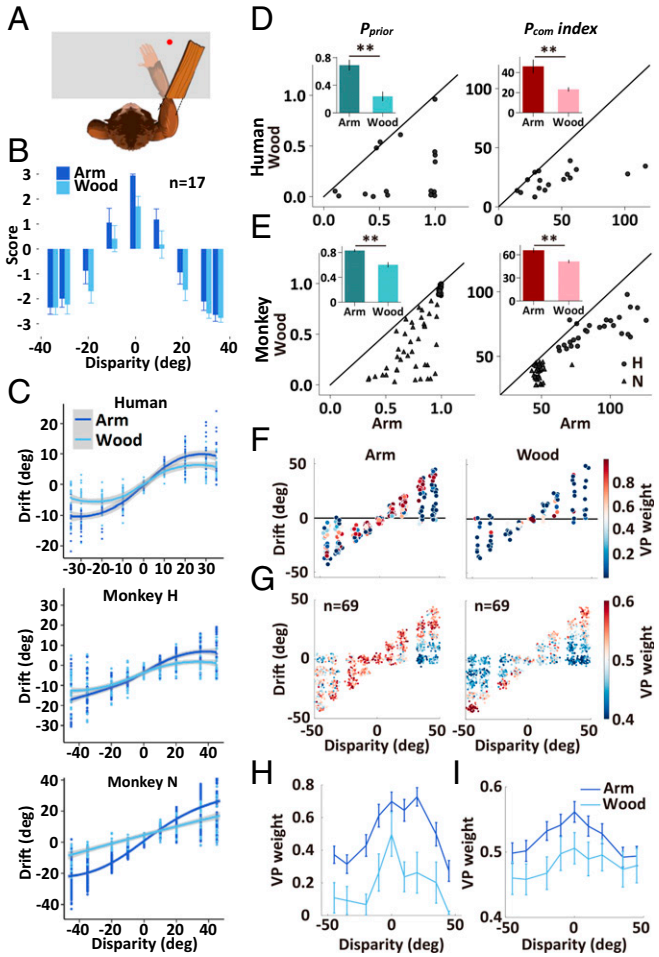

Fig. 4. Behavioral performance, model fittings, and premotor neural activities during the target-holding period in the wood experiment. (*A*) Overview of the task-performing platform showing the wood arm. (*B*) The ownership illusion score in both arm and wood conditions in the human questionnaire experiment. (*C*) Spatial drifts in the V arm and wood conditions. (*D* and *E*) BCI model fitting in the wood and arm conditions and plots of the prior (P_{prior}) and the index of posterior common source probabilities (P_{com}) (defined in Fig. 2*J*) in both humans ($n = 17$ participants) and monkeys ($n = 69$ sessions). The index was defined as the HWHM of the respective curves (Fig. 2*J*). (*F* and *H*) Plots of the example neuron of the VP weights of each trial under both V and wood conditions. (*G*) Pattern of VP weight in the population ($n = 69$) neural activity from 2 monkeys in both V arm and wood conditions. (*I*) Comparison of the dynamic of VP weight of the population neurons between the arm and the wood conditions. Error bars represent 1 SEM. $^{**}P < 0.01$.

Interestingly, the wood experiment was also a control for the sense of agency, which is the experience of controlling one's own motor acts (16) because, in both arm and wood conditions, subjects experienced controlling and moving the visual object, while the experience of the arm as one's own only existed in the arm condition (22, 25). Agency can readily be also experienced for noncorporal objects in the absence of a body ownership illusion (16). We then compared the agency ratings between the arm and the wood conditions and found no significant difference (*SI Appendix*, Fig. S11*A*, $F[1,16] = 0.01$, $P = 0.92$). Furthermore, the proprioceptive drifts did not show significant correlation with agency ratings in the arm condition (*SI Appendix*, Fig. S11*B*, Pearson correlation, $R = 0.30$, $P = 0.25$).

The breakdown of arm illusion was also revealed in the activities of premotor neurons. Recording of 126 neurons from the 2 monkeys showed that, during the target-holding period, the probabilities of integration (illusion) for the the wood condition

at both single-neuron (Fig. 4*F*) and population levels were significantly lower than those found in the arm condition (Fig. 4 *H* and *I*, ANOVA, single neurons: $P < 10^{-4}$; population: $P < 0.05$). These results support the notion that prior knowledge of body representation modulates the sense of arm illusion, presumably by selective integration of body-related versus nonbody V information in premotor neurons (2, 5, 6).

Discussion

We designed an experimental paradigm, using a video-based setup to probe the monkey's body representation and sense of ownership. We demonstrated that monkeys, similar to humans, integrated external stimuli as part of the self when P and V signals were coherent and tended to segregate the signals as the disparity progressively increased. In humans, we measured the arm ownership explicitly through oral reports and observed that these reports were tightly related to specific dynamics of the reaching behavior, which was predicted by the BCI model. In agreement with other human behavioral studies (15, 16), these results are the landmark of the process of hierarchical CI. This suggests that the hidden posterior common source probability accounts for the strength of arm illusion and should be reflected in subjective ratings of arm illusion. We then showed that neurons in the premotor cortex, both individually and synergistically as a population, can encode the dynamics of hidden probability of common source, update the posterior probability with the prior knowledge of body representation, and show consistent variability across trials as that predicted by the pattern of drift. Therefore, both behavioral and neural data in monkeys supported the recent theoretical work of body representation and self-consciousness (4, 24): the estimation of body position and the formation of body consciousness are determined by both the external properties of sensory inputs (the reliability of and disparity between V and P) and the internal prior body representation (the probability of same cause for V and P signals).

A Behavioral Paradigm for Arm Ownership. Our results differ from previous observations about body representation in animals. Earlier work demonstrated that synchronous stimulation of a monkey's unseen arm and a seen fake arm or visual exposure to the fake arm caused changes in the receptive fields of multimodal neurons in the premotor and parietal cortices (6, 7). Similarly, neurons in the primary somatosensory and motor cortices also changed their activities when synchronously touching the monkey's arm and an avatar arm (18). However, the animals in these studies were passively presented with visual or tactile stimuli without behavioral measurements of arm ownership. The present study reports nonhuman primates actively reporting their arm ownership in an active behavioral task and further expands previous human research exploring the CI in the rubber-hand illusion by examining the effect of prior body representation in the process of hierarchical inference (15).

Although the classic rubber-hand illusion was usually induced with a passive tactile stimulus (e.g., brush), several human experiments have shown that the participants could experience a physical moving model arm as their own arm just as illusory ownership is experienced in the traditional rubber-hand illusion (16). In fact, there is accumulating evidence that the body ownership and agency interact in producing ownership illusions (26–28). For example, Kokkinara and Slater (27) found a higher ownership for a virtual leg in active movement than synchronous passive V–tactile stimulation conditions.

Arm illusions in humans have been mostly studied either through explicit reports using subjective ratings and questionnaires or using objective measurements of proprioceptive drift (1, 3, 16). Other researchers have found no causal link between the subjective rating and the proprioceptive drift and have argued that they measure different core processes that underpin the subjective feeling of arm ownership (29, 30). For example, changes in proprioceptive drift have been observed without changes in ownership (29). This means that there may be other factors and sources which can affect drift but does not imply that the subjective rubber-hand illusion cannot cause proprioceptive drift (30). However, the ownership in the current study is most likely the cause of proprioceptive drift by the objective measurement, which was well fitted and predicted by the BCI model.

Neural Correlates of Monkey Premotor Cortex in Multisensory Integration of Arm Ownership. The activity in single neurons in the premotor cortex which we observed in this study is consistent with previous experiments conducted in humans, which have shown that brain activity in the premotor cortex correlates with the strength of the rubber-hand illusion and similar arm ownership illusions (5, 9, 10, 21). Our results are also consistent with a human electrocorticogram study, that showed sustained high-γ activity in the premotor cortex reflected the feeling of ownership during the rubber-hand illusion. Instead, high-γ activity locked to the tactile stimulus (but not to the illusion itself) was more closely localized to the posterior cortex (31).

Our results are also consistent with previous findings by Graziano and colleagues, showing that the visual receptive fields of premotor neurons were shifted along with the monkey's P arm (6), and the P spatial tuning was changed to the location of the fake visual arm (7). This establishes a natural relation between the P_{com} and the tuning curves, however, it has to be noted that even neurons without spatial tuning can contribute to P_{com} computation as long as their activities under the conflict condition show a difference from the integration (VP condition) or segregation (P condition). Therefore, our study presents a linear probabilistic model capable of computing the probability of integration and segregation at the single-neuron and single-trial levels.

Furthermore, while we could not fully discard that premotor activity showing the CI pattern might represent a combination of agency and ownership, we could affirm that these neurons cannot solely represent agency as there was significant differential activity at both single- and population-neuron levels between the arm and the wood conditions.

Proposal of Neural Dynamics for CI of Bodily Self-Consciousness. With the evidence at this stage, we speculate on how the activity we observed in the premotor cortex may participate in an extended network involved in the formation of body representation. We suggest that the body representation may lie in a dynamic loop of the frontal–parietal interactions. Specifically, premotor neurons carry information to discriminate between 2 causes or a single cause and can then provide feedback to each specific sensory area (primary somatosensory, area 5, and visual cortex) that, in turn, encode distribution of properties of attribute of an entity (e.g., its position and shape) which is then used to recalibrate sensory signals for the estimation of a body in space. The idea that sensory signals feed to the frontal cortex that makes an inference and, in turn, this information is fed back to set priors which subsequently organize the encoding and inference of sensory integration, is reminiscent of cognitive models of perception and consciousness (4, 24, 32). Future studies could examine how the distinct population of neurons in different brain regions (e.g., area 5 and the somatosensory cortex) correlate with the other estimates in the framework of BCI (e.g., the neural representation of the prior and likelihood) (13) and how other body constraints (e.g., peripersonal space, embodiment, and interoception) contribute to the neural representation of bodily self (2, 32).

Furthermore, the parallel that we could establish in behavioral studies of human and nonhuman primates together with in vivo recording from the monkey brain illustrate the usefulness of nonhuman primates in studying the neural basis of bodily self-consciousness and may ultimately allow exploring the mechanisms of impaired self-knowledge in neurological diseases, such as body delusions and developing of neuroprosthetic arms that belong to one's own body (33).

Materials and Methods

Data for these experiments were collected from 4 adult male rhesus monkeys (*Macaca mulatta*) and 25 human subjects. All animal and human experimental

procedures were approved by the ethical committee of the Institute of Neuroscience, Shanghai Institutes for Biological Sciences, Chinese Academy of Sciences (CAS). Informed written consent was obtained from all human subjects. Full details of our task design, neurophysiological recordings, and analysis are provided in the *SI Appendix*.

ACKNOWLEDGMENTS. We thank Mu-ming Poo, Stanislas Dehaene, Patrick Haggard, and Tianming Yang for their comments on the manuscript, and Dora E. Angelaki and Yond-Di Zhou for their suggestions on data analysis, and Xinjian Jiang, Jian Jiang, and Jing Wu for experimental assistance. This work was supported by the Key Research Program of Frontier Sciences QYZDY-SSW-SMC001, the Strategic Priority Research Programs XDB32070200 and XDB32010300, the CAS Pioneer Hundreds of Talents Program, the Shanghai Municipal Science and Technology Major Project 2018SHZDZX05, and the Shanghai Key Basic Research Project 16JC14202001 to L.W.

1. H. H. Ehrsson, "The concept of body ownership and its relation to multisensory integration" in *The New Handbook of Multisensory Processing*, B. E. Stein, Ed. (Mit Press, 2012), pp. 775–792.
2. O. Blanke, M. Slater, A. Serino, Behavioral, neural, and computational principles of bodily self-consciousness. *Neuron* **88**, 145–166 (2015).
3. M. Botvinick, J. Cohen, Rubber hands 'feel' touch that eyes see. *Nature* **391**, 756 (1998).
4. K. Kilteni, A. Maselli, K. P. Kording, M. Slater, Over my fake body: Body ownership illusions for studying the multisensory basis of own-body perception. *Front. Hum. Neurosci.* **9**, 141 (2015).
5. H. H. Ehrsson, C. Spence, R. E. Passingham, That's my hand! Activity in premotor cortex reflects feeling of ownership of a limb. *Science* **305**, 875–877 (2004).
6. M. S. A. Graziano, Where is my arm? The relative role of vision and proprioception in the neuronal representation of limb position. *Proc. Natl. Acad. Sci. U.S.A.* **96**, 10418–10421 (1999).
7. M. S. Graziano, D. F. Cooke, C. S. Taylor, Coding the location of the arm by sight. *Science* **290**, 1782–1786 (2000).
8. B. Pesaran, M. J. Nelson, R. A. Andersen, Dorsal premotor neurons encode the relative position of the hand, eye, and goal during reach planning. *Neuron* **51**, 125–134 (2006).
9. H. H. Ehrsson, N. P. Holmes, R. E. Passingham, Touching a rubber hand: Feeling of body ownership is associated with activity in multisensory brain areas. *J. Neurosci.* **25**, 10564–10573 (2005).
10. C. Brozzoli, G. Gentile, H. H. Ehrsson, That's near my hand! Parietal and premotor coding of hand-centered space contributes to localization and self-attribution of the hand. *J. Neurosci.* **32**, 14573–14582 (2012).
11. M. S. A. Graziano, M. M. Botvinick, How the brain represents the body: Insights from neurophysiology and psychology. *Attention Perform* **19**, 136–157 (2002).
12. M. O. Ernst, M. S. Banks, Humans integrate visual and haptic information in a statistically optimal fashion. *Nature* **415**, 429–433 (2002).
13. K. P. Körding *et al*., Causal inference in multisensory perception. *PLoS One* **2**, e943 (2007).
14. T. Rohe, U. Noppeney, Cortical hierarchies perform Bayesian causal inference in multisensory perception. *PLoS Biol.* **13**, e1002073 (2015).
15. M. Samad, A. J. Chung, L. Shams, Perception of body ownership is driven by Bayesian sensory inference. *PLoS One* **10**, e0117178 (2015).
16. A. Kalckert, H. H. Ehrsson, Moving a rubber hand that feels like your own: A dissociation of ownership and agency. *Front. Hum. Neurosci.* **6**, 40 (2012).
17. M. Tsakiris, P. Haggard, The rubber hand illusion revisited: Visuotactile integration and self-attribution. *J. Exp. Psychol. Hum. Percept. Perform.* **31**, 80–91 (2005).
18. S. Shokur *et al*., Expanding the primate body schema in sensorimotor cortex by virtual touches of an avatar. *Proc. Natl. Acad. Sci. U.S.A.* **110**, 15121–15126 (2013).
19. C. Brozzoli, G. Gentile, V. I. Petkova, H. H. Ehrsson, FMRI adaptation reveals a cortical mechanism for the coding of space near the hand. *J. Neurosci.* **31**, 9023–9031 (2011).
20. J. Vergara, N. Rivera, R. Rossi-Pool, R. Romo, A neural parametric code for storing information of more than one sensory modality in working memory. *Neuron* **89**, 54–62 (2016).
21. G. Gentile, A. Guterstam, C. Brozzoli, H. H. Ehrsson, Disintegration of multisensory signals from the real hand reduces default limb self-attribution: An fMRI study. *J. Neurosci.* **33**, 13350–13366 (2013).
22. M. Tsakiris, L. Carpenter, D. James, A. Fotopoulou, Hands only illusion: Multisensory integration elicits sense of ownership for body parts but not for non-corporeal objects. *Exp. Brain Res.* **204**, 343–352 (2010).
23. M. R. Longo, F. Schüür, M. P. Kammers, M. Tsakiris, P. Haggard, What is embodiment? A psychometric approach. *Cognition* **107**, 978–998 (2008).
24. J. P. Noel, O. Blanke, A. Serino, From multisensory integration in peripersonal space to bodily self-consciousness: From statistical regularities to statistical inference. *Ann. N. Y. Acad. Sci.* **1426**, 146–165 (2018).
25. A. Guterstam, G. Gentile, H. H. Ehrsson, The invisible hand illusion: Multisensory integration leads to the embodiment of a discrete volume of empty space. *J. Cogn. Neurosci.* **25**, 1078–1099 (2013).
26. D. Burin *et al*., Are movements necessary for the sense of body ownership? Evidence from the rubber hand illusion in pure hemiplegic patients. *PLoS One* **10**, e0117155 (2015).
27. E. Kokkinara, M. Slater, Measuring the effects through time of the influence of visuomotor and visuotactile synchronous stimulation on a virtual body ownership illusion. *Perception* **43**, 43–58 (2014).
28. M. Tsakiris, G. Prabhu, P. Haggard, Having a body versus moving your body: How agency structures body-ownership. *Conscious. Cogn.* **15**, 423–432 (2006).
29. M. Rohde, M. Di Luca, M. O. Ernst, The rubber hand illusion: Feeling of ownership and proprioceptive drift do not go hand in hand. *PLoS One* **6**, e21659 (2011).
30. Z. Abdulkarim, H. H. Ehrsson, No causal link between changes in hand position sense and feeling of limb ownership in the rubber hand illusion. *Atten. Percept. Psychophys.* **78**, 707–720 (2016).
31. A. Guterstam *et al*., Direct electrophysiological correlates of body ownership in human cerebral cortex. *Cereb. Cortex* **29**, 1328–1341 (2019).
32. A. K. Seth, M. Tsakiris, Being a beast machine: The somatic basis of selfhood. *Trends Cogn. Sci. (Regul. Ed.)* **22**, 969–981 (2018).
33. K. L. Collins *et al*., Ownership of an artificial limb induced by electrical brain stimulation. *Proc. Natl. Acad. Sci. U.S.A.* **114**, 166–171 (2017).